

Rare Event Simulation of a Rotorcraft System

Benjamin J. Zhang* and Youssef M. Marzouk†
Massachusetts Institute of Technology, Cambridge, MA 02139

Byung-Young Min‡
United Technologies Research Center, Hartford, CT, 06108

Tuhin Sahai §
United Technologies Research Center, Berkeley, CA, 94705

We demonstrate an algorithm for efficient rare event sampling in a rotorcraft model. Helicopter design parameters are typically chosen for efficient performance in cruise and hover. At the same time, structural components such as the length of the tail are chosen so that the rotorcraft is stable under perturbation by environmental factors such as noisy wind. In the face of stochastic forcing, however, environmental conditions may still lead to rare accidents despite good engineering design. We adapt a recent dynamic importance sampling algorithm for small-noise diffusions, derived from the theory of large deviations, to efficient sampling of rare events in a model rotorcraft system. The method achieves variance reduction in estimating the probabilities of stall events, and helps identify the dynamics leading to these phenomena.

I. Nomenclature

$\mathcal{AC}([t, t_f]; \mathbb{R})$	= Space of \mathbb{R} -valued absolutely continuous functions on $[t, t_f]$.
A_t	= Tail airfoil area
a, b, c	= Parameters of the linearized model
$b(x)$	= Deterministic system dynamics
C_d	= Coefficient of drag
C_l	= Coefficient of lift
C_{l_α}	= Tail lift coefficient approximate model
C_{M-x}	= Normalized hub roll moment
C_{M-y}	= Normalized hub pitching moment
C_Q	= Torque
C_T	= Coefficient of thrust
C_X	= Drag or propulsive force
$C_{l_{\alpha_0}}$	= Lift coefficient with zero angle of attack
$\mathcal{C}_0([0, t_f])$	= Space of continuous functions on $[0, t_f]$
E	= Rare event set of interest
f	= Airfoil table lookup function
H	= Hamiltonian of Hamilton-Jacobi equation
$I(\cdot)$	= Large deviations rate function
I_y	= Aircraft moment of inertia
L_H	= Lift from horizontal tail airfoil
L/D_e	= Rotor performance

*Graduate Student, Department of Aeronautics and Astronautics, bjz@mit.edu, AIAA Student Member.

†Associate Professor, Department of Aeronautics and Astronautics, ymarz@mit.edu, AIAA Associate Fellow.

‡Staff Research Engineer, currently at Sikorsky, A Lockheed Martin Company, byung.young.min@lmco.com, AIAA Member.

§Associate Director, sahait@utrc.utc.com

$\mathcal{L}(\mathbf{V}, \dot{\mathbf{V}})$	= Local large deviation rate function
M_{CG}	= Net moment around center of gravity
M_R	= Moment around rotor hub
M_n	= Mach number
M_{tip}	= Tip Mach number
q	= Rate of pitch
r	= Section radial location
T	= Rotor thrust
t	= Time
t_f	= Final time
$U(t, x)$	= Solution to Hamilton-Jacobi equation
$\mathbf{u} = [u_x, u_z]^T$	= Biasing function
$\mathbf{V} = [V_x, V_z]^T$	= Freestream velocity
\mathbf{V}_0	= Mean freestream velocity
V_i	= Induced velocity
\mathbf{W}_t	= Standard Brownian motion
$\mathbf{X}^\epsilon(t)$	= Dynamical system state
Z_E	= Importance weight
α	= Blade angle of attack
α_s	= Shaft angle of attack
α_t	= Tail airfoil angle of attack
$\beta_0, \beta_{1C}, \beta_{1S}$	= Blade flapping
Δs_H	= Distance from center of gravity to tail airfoil
Δs_R	= Distance from center of gravity to rotor hub
ϵ	= Noise parameter
$\theta = \theta(t)$	= Aircraft pitch angle
θ_0	= Collective pitch angle
θ_{1C}, θ_{1S}	= Cyclic pitch angles
θ_{bl}	= Blade pitch angle
θ_{el}	= Elastic deflection
θ_{tw}	= Blade twist angle
μ	= Advance ratio
$\hat{\rho}_E$	= Monte Carlo estimate
σ	= Diffusion matrix
σ_x, σ_z	= Diagonal components of the diffusion matrix
ψ	= Azimuth angle
Ω	= Blade rotational speed
$\omega_{C_l}, \omega_{C_d}$	= Uncertainty weighting factor in coefficients of lift and drag
$\mathbb{1}_E(\cdot)$	= Indicator function

II. Introduction

HELICOPTERS are typically designed for efficient performance in cruise conditions and in hover. At the same time, structural components and blades are sized based on extreme desired capabilities such as maximum thrust, maximum speed, and maneuverability. At the limits of rotor thrust and speed capabilities, the rotor may enter regions of instability, stall, increased power and increased vibratory loads. The occurrence of these conditions reduces the life of the rotorcraft and, in extreme circumstances, can lead to accidents. The extreme events of stall, loss of lift, and vibratory loads are very difficult to predict, particularly because these events lie in the tails of distributions and occur infrequently. These events are also subject to variability of the blade properties and specific flight conditions. An ultimate goal in rotorcraft engineering is to predict such events in a real time and online setting. Achieving this goal will enable autonomous vehicles to constantly monitor surroundings and ensure that the probability of catastrophic failure does not exceed a predetermined threshold. Taking cues from past work in rare event simulation and prediction [1, 2], we must find ways to

efficiently sample rare events before we study the online prediction of rare events. Therefore, in this paper we consider rare event simulation.

Rare event simulation involves estimating probabilities of unlikely events (usually on the order of 10^{-3} , often times much smaller [3]), estimating conditional expectations given a rare event has occurred, and characterizing distributions and dynamics conditioned on a rare event. There are two ingredients one needs to accurately study rare events of an engineering system. The first is a sufficiently faithful probabilistic model that can exhibit the rare events of interest with the correct probabilities. The resulting probability distributions induced by the model are often intractable to work with analytically, either because they cannot be easily expressed in terms of some canonical family, or because they are high dimensional. For practical computations, Monte Carlo simulations comprise the usual class of methods that are used to estimate expectations of interest. However, for estimating expectations sensitive to rare events, Monte Carlo estimates will require many samples to achieve a high quality (low variance) estimate. By a rough definition, rare events do not occur in simulation very often. For example, when simulating an event whose probability is on the order of 10^{-6} , on average, one will need to generate one million samples to obtain one realization of the rare event. Furthermore, to obtain a good estimate of the probability, one will require many more instances of the event. When one has a high fidelity model, in which the computational cost per sample is large, one may be hard pressed to retrieve even a few hundred samples.

Therefore, we can see that the second ingredient necessary for rare event simulation is a good methodology that retrieves samples from the rare event of interest efficiently. State-of-the-art rare event simulation methodology rely on variance reduction methods [4]. Importance sampling is one of the most common variance reduction techniques for rare event simulation. Importance sampling produces higher quality samples by generating them from a different distribution, called the biasing distribution, such that the rare event of interest occurs more frequently [4, 5]. Each sample is then re-weighted according to its relative importance with respect to the original distribution.

While there exists a large collection of methods for rare event simulation, e.g. conditional Monte Carlo [4, 6], the cross-entropy method [7], information theoretic bounds [8], etc., one of the broadest and most unifying approaches leverages the theory of large deviations [9–11]. Large deviations theory arises from the desire to find refinements of the laws of large numbers. The theory provides a set of tools for a computer-less mathematician to study rare events and provides alternative ways of comparing and quantifying rarity of events without the exact probability values.

Using the rich set of theoretical techniques from large deviations, past research has provided a computational paradigm for constructing good importance sampling estimators for rare event simulation [12]. One of the key insights that allowed large deviations to provide a unifying framework for rare event simulation is through a control-theoretic approach to the classical theory [10]. Recent work in dynamic importance sampling [13] has shown a way of finding good importance sampling distributions through differential game and control theoretic interpretations which amounts to finding the solution to an Isaacs partial differential equation. For rare event simulation, this equation was shown to be equivalent to a Hamilton-Jacobi PDE or a collection of variational problems. While many past methods were tailored to specific classes of problems, this control-theoretic approach to large deviations and rare event simulation admitted a general framework that easily adapted to large classes problems including small noise diffusions [2].

The goal of this paper is to demonstrate a recent method for rare event simulations of diffusions by testing it on a model rotorcraft system. The main question we address is: given a well designed rotorcraft system in cruise that is perturbed by noisy wind modeled as a small noise diffusion, what is the probability that the magnitude of the rotorcraft pitch angle will exceed some value within some fixed time frame? We will answer this question with state-of-the-art rare event simulation techniques.

The rest of the paper is organized as follows. In Section III, we give a description of the rotorcraft model we consider, and show a few simulations to explore the rare event of interest. In Section IV, we review the theory of efficient importance sampling methodology and present the algorithm we are using. In Section V, we apply the algorithm to the problem at hand. Finally, we provide some discussion of the efficacy of the method, future work, and conclude the paper in Section VI.

III. The rotorcraft model

In this section, we formulate the rotorcraft model. We use a rigid beam rotor analysis code called GENTRIM [14]. It is designed for fast rotor performance analysis based on blade element methods (BEM) and includes a trim control solver. Airfoil tables are used for section aerodynamics. We use the publicly available NACA0012 airfoil data for the airfoil table. For high fidelity aerodynamics, the model can be coupled with computational fluid dynamics code. In this paper, the aerodynamics is only based on airfoil table data and surrogate models. Typically, a uniform induced velocity is used and blade flapping dynamics can easily be included. With given flight (ambient) and rotor conditions (such as RPM, desired thrust and hub moments), GENTRIM trims the rotor with cyclic control inputs ($\theta_0, \theta_{1C}, \theta_{1S}$), and outputs corresponding performance metrics (such as rotor torque, propulsive force, and lift over drag ratio). A summary of its input and output variables are given in Table 1.

When the aerodynamics of the model is based on airfoil tables, the fidelity of the aerodynamic forces depend on the airfoil table resolution. Fine resolution of the Mach number and angle of attack lead to more accurate predictions of aerodynamic forces. Additionally, stall characteristics can also be included in the airfoil tables. While GENTRIM does not include aeroelastic modeling, the source code is fully accessible to the user. Therefore any necessary modifications to the states for performing online updates can be made relatively easily.

Simple vehicle dynamics can be included for angle of attack stability analysis. Typically, helicopters are unstable in response to upward gusts during forward flight. The upward gusts (V_z) cause a higher angle of attack, which increases rotor thrust. If the thrust vector is located ahead of the fuselage CG point, the increased thrust produces a nose-up pitching moment. The nose-up attitude further increases the rotor disk angle of attack, hence leading to an instability. Even if the thrust vector is located behind the fuselage CG point, the rotor flapping dynamics makes the high angle of attack lead blade to tilt backwards due to the asymmetry in dynamic pressure in the advancing and retreating sides. This effect also contributes to destabilization. To mitigate stability issues, we require the net pitching moment (M_{CG}) to be such that $M_{CG}/\partial V_z < 0$. To this end, a horizontal tail with an airfoil is introduced to balance the pitching moment of the rotor. The simplified equations of motion can be expressed as:

$$\begin{aligned}\dot{\theta} &= q, \\ \dot{q} &= \frac{M_{CG}}{I_y}, \\ M_{CG} &= M_R + Tds_R - L_H ds_H.\end{aligned}\tag{1}$$

In the above equations, θ is the pitch of the rotorcraft, q is the pitch rate, M_R is the moment around the rotor hub, Tds_R is the moment due to rotor thrust, and $L_H ds_H$ is the moment due to lift from the horizontal tail. Thus, depending on the size of the horizontal tail, rotor characteristics, and flight conditions, a vehicle can, under certain conditions, encounter instabilities and potentially crash. To convey the complexity of the model and the variables we are considering, we refer the reader to Table 1 and to Figure 1. Figure 1 pictorially shows how the model parameters and variables depend on each other.

A. Rotor Blade Element Method (BEM)

The GENTRIM code evaluates rotor thrust, torque, horizontal force, roll and pitch hub moments, and rotor lift over drag ratio L/D_e with given input parameters using the blade element method (BEM). It can also trim the rotor for specified thrust and hub moments, and outputs pitch control settings. The blade element method is used to compute integrated hub forces and moments. At a given blade section (Figure 2), the

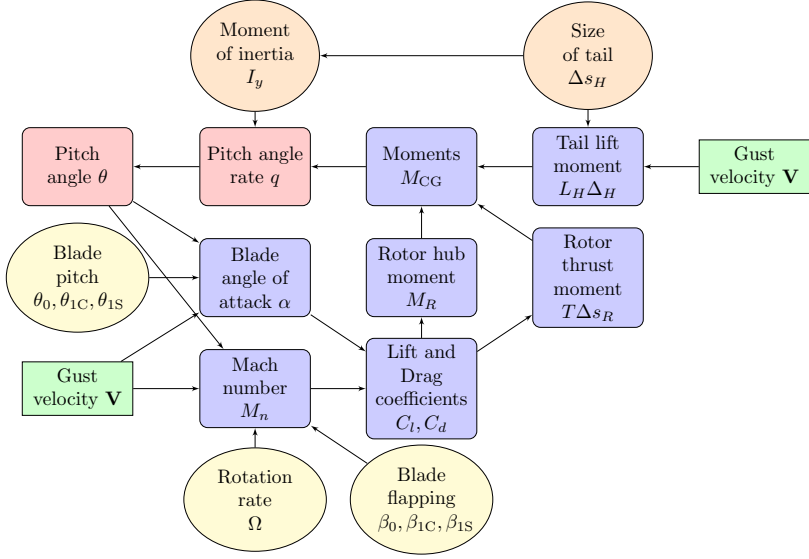


Fig. 1 Schematic of rotorcraft model and their interdependencies.

I/O	Variable Type	Variable	Description
Inputs	Geometry	Radius	Blade radius
		Twist distribution	Blade twist distribution
		Chord distribution	Blade chord length distribution
	Operating Condition	Airfoil table ($C_l, C_d = f(M_{tip}, \alpha)$)	C81 table for each airfoil, containing C_l and C_d as function of Mach number and angle of attack
		M_{tip}	Tip Mach number
		C_T	Rotor thrust coefficient
		C_{M-x}	Hub roll moment (+ starboard up)
		C_{M-y}	Hub pitching moment (+ nose up)
		Pressure	Ambient pressure
	Flight Condition	Temperature	Ambient temperature
		μ	Advance ratio $\frac{V_\infty}{V_{Tip}}$
		α_s	Shaft angle of attack
Outputs	Forces/Moments	C_Q	Torque
		C_X	Drag or propulsive Force
	Blade Pitch Control	$\theta_0, \theta_{1C}, \theta_{1S}$	$\theta_{bl} = \theta_0 + \theta_{1C} \cos(\psi) + \theta_{1S} \sin(\psi)$
	Blade Flapping	$\beta_0, \beta_{1C}, \beta_{1S}$	$\beta = \beta_0 + \beta_{1C} \cos(\psi) + \beta_{1S} \sin(\psi)$
	Rotor Performance	L/D_e	$\frac{L}{D_e} = \frac{C_L}{C_H + C_Q/\mu}$

Table 1 Parameters of the rotorcraft and trim model. The input and output variables of the trim control are labeled accordingly.

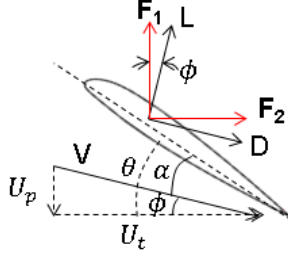


Fig. 2 Airfoil section pitching.

normal and tangential forces are computed as follows,

$$\begin{aligned} \alpha &= \theta - \phi, \\ U_p &= V_i \cos(\beta) + r\dot{\beta} + V_x \cos(\alpha_s) \sin(\beta) \cos(\psi) - V_x \sin(\alpha_s) \cos(\beta) - V_z \cos(\alpha_s) \cos(\beta), \\ U_t &= \Omega r \cos(\beta) + V_x \cos(\alpha_s) \sin(\psi) - V_z \sin(\alpha_s) \sin(\psi), \\ C_l, C_d &= f(\alpha, M, \omega_{C_l}, \omega_{C_d}), \\ F_1 &= C_l \cos(\phi) - C_d \sin(\phi), \\ F_2 &= C_l \sin(\phi) + C_d \cos(\phi). \end{aligned} \quad (2)$$

Here, α is the angle of attack, V_i is the induced velocity, β is the blade flapping angle, ψ is the azimuth angle, α_s is the shaft angle of attack, M is the Mach number, Ω is the blade rotational speed, r is the section radial location, V_x and V_z are freestream velocity components, and ω_{C_l} and ω_{C_d} are uncertainty weighting factor. In this paper, there is no uncertainty when computing the coefficients of lift and drag. This model feature may be considered for future research. The blade pitch angle is described using the following equation,

$$\theta = \theta_0 + \left(\frac{r}{R} - 0.75 \right) \theta_{tw} + \theta_{1s} \sin(\psi) + \theta_{1c} \cos(\psi) + \theta_{el}, \quad (3)$$

where, θ_0 is the collective pitch angle, θ_{tw} is the twist angle, θ_{1s} and θ_{1c} are the cyclic pitch angles, and θ_{el} is the elastic deflection. Once section F_1 and F_2 forces are computed, integrated hub loadings at a given azimuth angle are computed as

$$\begin{aligned} \text{Thrust} &= \int_{r_0}^{\text{Tip}} F_1 \cos(\beta) dr, \\ \text{Torque} &= \int_{r_0}^{\text{Tip}} F_2 r \cos(\beta) dr. \end{aligned} \quad (4)$$

To compute the induced velocity on the rotor blades, a linear inflow model is used as shown in following expressions

$$\begin{aligned} \frac{V_i}{V_{\text{tip}}} &= \lambda_0 (1 + k_x \cos(\psi) + k_y r \sin(\psi)), \\ \lambda_0 &= \frac{C_T}{2\sqrt{\mu^2 + (\mu \tan(\alpha_s) + \lambda_0)^2}}, \end{aligned} \quad (5)$$

where C_T is the thrust coefficient and μ is the advance ratio which is given as,

$$\mu = \frac{V_\infty \cos(\alpha_s)}{V_{\text{tip}}}. \quad (6)$$

The second equation for λ_0 is solved using Newton iterations for given thrust and advance ratio conditions. The lift from the horizontal tail is computed as

$$L_H = \frac{1}{2} (V_x^2 + V_z^2) A_t C_{l\alpha} \alpha_t, \quad (7)$$

where A_t is the area of the tail airfoil. To determine the lift coefficient of the tail airfoil, we use an affine model $C_l = C_{\alpha_0} + C_{l_\alpha} \alpha_t$, where C_{α_0} is the lift coefficient when the angle of attack is zero. We model stall of the airfoil by cutting off the lift coefficient past $\pm 15^\circ$. That is, any angle of attack outside $\pm 15^\circ$ has zero lift coefficient. While in reality, the angle of attack does not go to zero immediately outside this region, we model it as described since we do not simulate the rotorcraft for angles of attack outside this range. For an approximation to the NACA0012 airfoil we have $C_{l_\alpha} = 2\pi$. For detailed equations for rotor blade element method we refer the reader to [15, 16].

B. Exploring the rare events

In this section, we simulate a few model runs to qualitatively explore conditions that may cause a helicopter in cruise to experience stall in its horizontal tail airfoil and therefore cause the helicopter to become unstable. In following simulations, the parameters of the rotorcraft are chosen according to the specifications of an MBB Bo 105 helicopter [17]. We first only consider rare events caused by random gusts, or noisy wind. The noise in the wind is modeled as an Ornstein-Uhlenbeck process, which is a mean reverting diffusion process. This is a continuous model of wind speeds where it is a constant value on average, and noise is driven by a Brownian motion. See [18] for a more thorough discussion on wind models. The wind is expressed as the following stochastic differential equation

$$d\mathbf{V} = (\mathbf{V}_0 - \mathbf{V}) dt + \sigma d\mathbf{W}_t \quad (8)$$

where $\mathbf{V} = [V_x, V_z]^T$, the x and z velocities of the helicopter relative to the ground, \mathbf{V}_0 is the mean velocity, σ is the diffusion matrix, and \mathbf{W}_t is a standard two dimensional Brownian motion. In the following simulations, the diffusion matrix is of the form

$$\sigma = \begin{bmatrix} \sigma_x & 0 \\ 0 & \sigma_z \end{bmatrix}.$$

Physically this models that the vertical gusts are independent of the horizontal gusts.

For all the simulations, we trim the system so that the helicopter generating enough lift to keep it in the air while cruising horizontally at a speed of approximately 44.2 meters per second (99 mi/hr), with zero vertical speed. That is, we desire the hub roll and pitch moments, C_{M-x} and C_{M-y} respectively, to be zero, while having the mean velocity to be equal to $\mathbf{V}_0 = [44.2, 0]$ m/sec. By trimming, we mean finding the blade pitch controls $\theta_0, \theta_{1C}, \theta_{1S}$ that achieve these desired flight conditions. The pitch of the aircraft is tilted forward at 0 degrees from the horizontal, so it is level with the ground. We show a few plots of the evolution the pitch over time under noisy wind conditions. We numerically integrate the system forward in time using a simple Euler-Maruyama solver [19].

In the following figures we show plots of the time evolution of the helicopter pitch under varying noisiness in the wind and sizes of the horizontal tail. Recall that in our model, the horizontal tail has an airfoil which stabilizes the rotorcraft, and that airfoil angle may exhibit stall when the vehicle pitch angle is outside the range $-15^\circ \leq \theta \leq 15^\circ$. Therefore, we are looking for environmental and design conditions such that the pitch will fall outside that value. In Figure 3, we show the time evolution of the pitch of the helicopter system while being perturbed by the noise from the wind. We plot θ and the velocity profiles as functions of time with no further trimming or other control mechanism over the course of the simulation. Here we have $\sigma_x = 0.55$ m/sec (1.23 mi/hr) and $\sigma_z = 0.55$ m/sec (1.23 mi/hr).

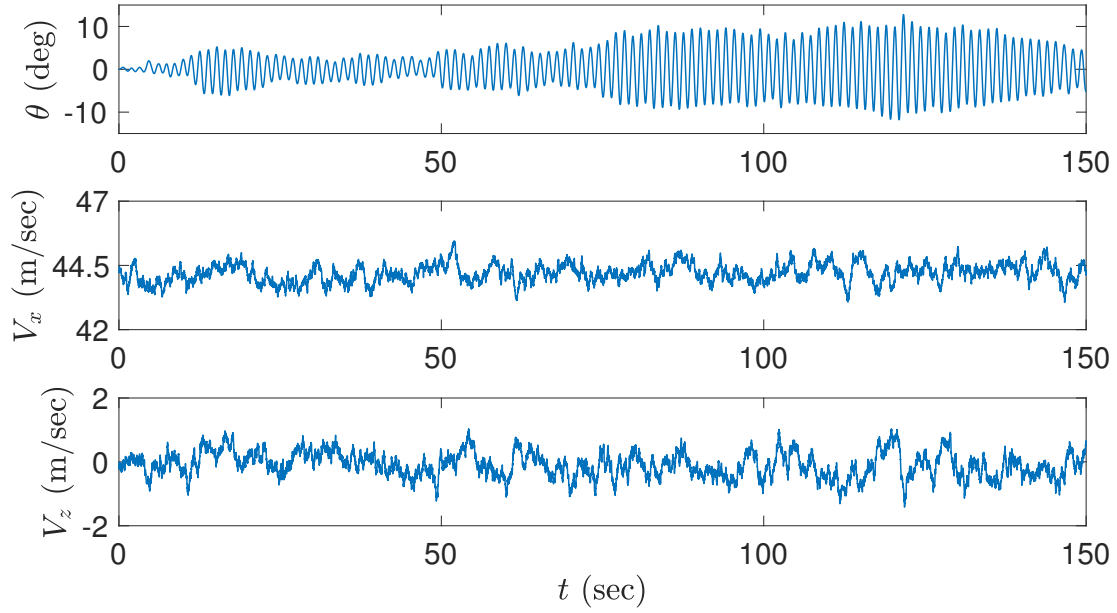


Fig. 3 Evolution of the pitch angle θ over time with noise in both the horizontal and vertical velocities. We have $\sigma_x = 0.55$ m/sec, $\sigma_z = 0.55$ m/sec and $\Delta s_H = 4.7$ meters.

Figure 4 shows that with a larger entries in the diffusion matrix of the noise in the wind, the helicopter becomes less stable. We see that the pitch angle exceed 15° and becomes unstable. Here we have $\sigma_x = 4.42$ m/sec (10 mi/hr) and $\sigma_z = 2.76$ m/sec (6.2 mi/hr).

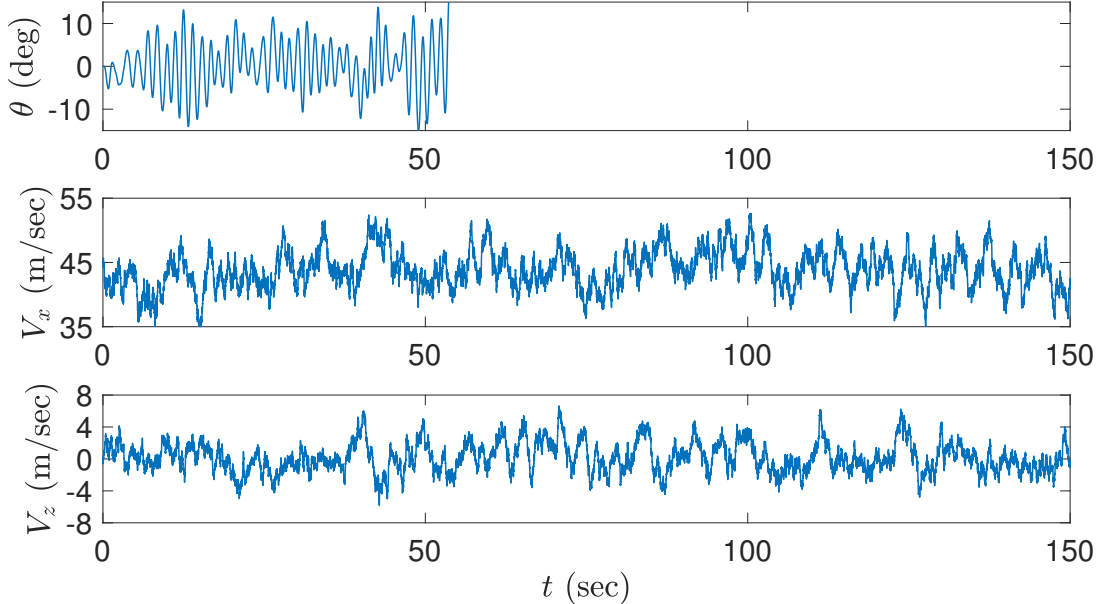


Fig. 4 Under noisier, larger variance, the helicopter has larger oscillations. We have $\sigma_x = 4.42$ m/sec, $\sigma_z = 2.76$ m/sec and $\Delta s_H = 4.7$ meters.

Figure 5 shows how larger oscillations form when the tail is half the size of the usual tail length. Eventually

the sample paths leave the region of stability. Here we have $\sigma_x = 0.55$ m/sec and $\sigma_z = 0.55$ m/sec.

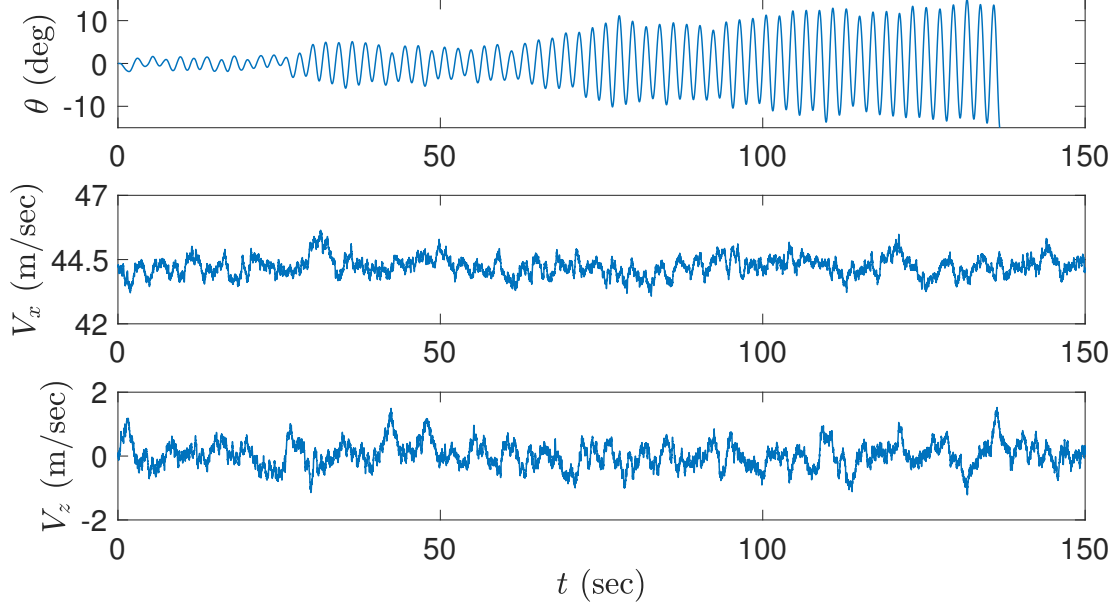


Fig. 5 The helicopter with a shorter tail has larger oscillations, so it is less stable. We have $\sigma_x = 0.55$ m/sec, $\sigma_z = 0.55$ m/sec and $\Delta s_H = 2.35$ meters.

Given these simulations, a dangerous event can be defined as the helicopter pitch angle exceeding $\pm 15^\circ$. The reasoning is that since the tail airfoil is used to stabilize the rotorcraft in flight, it will fail produce lift beyond this range as the airfoil will stall. This will cause the helicopter to become unstable. Realistically, a pilot cannot apply control by trimming the helicopter continuously in time and reacting to large unexpected events. What is more likely is that the pilot can only apply trim control to the rotorcraft once every few seconds. Therefore, the rare event we define is that the helicopter pitch angle exceeds $\pm 15^\circ$ within some fixed time period. What makes this event rare is that usually one designs the tail such that the wind that causes this instability does not happen often.

In the next sections, we will review a rare event simulation methodology for small noise diffusions and then apply the method to the problem we have defined.

IV. Reviewing rare event simulation of small noise diffusions

For efficient rare event simulation, we consider the variance reduction method of importance sampling. One is usually familiar with constructing biasing distributions for \mathbb{R}^d -valued distributions or a sequence of biasing distributions for discrete time Markov chains. How to perform importance sampling for diffusions is less clear. One valid approach is to discretize the stochastic differential equation model at hand first to obtain a discrete time Markov chain and then construct a sequence of biasing distributions at each time step. This approach can be thought of as a *discretize then bias* approach. Here we state a theorem from stochastic calculus that allows one to find a biasing function first, before performing any discretization. This involves first finding a biased stochastic differential equation model that reaches the rare event more often, then simulate the biased SDE by discretizing the system. For diffusions, they are equivalent in the limit as the discretization become finer. Girsanov's theorem allows one to find the importance weight between the biased and unbiased diffusions. The full statement of Girsanov's theorem contains many technical minutiae, and we strongly recommend the reader to consult further resources related to the details of the theorem [20].

Theorem IV.1 (Girsanov) Let \mathbf{X}^ϵ be the solution to the stochastic differential equation evolving on \mathbb{R}^d

for $t \in [0, t_f]$

$$\begin{aligned} d\mathbf{X}^\epsilon(t) &= b(\mathbf{X}^\epsilon(t))dt + \sqrt{\epsilon}\sigma(\mathbf{X}^\epsilon(t))d\mathbf{W}_t \\ \mathbf{X}^\epsilon(0) &= \mathbf{x}_0 \end{aligned} \quad (9)$$

which induces a probability measure \mathbb{P} , where \mathbf{W}_t is a standard Brownian motion on \mathbb{R}^d . Suppose \mathbb{P}^u is a probability measure induced by the SDE for $t \in [0, t_f]$

$$\begin{aligned} d\tilde{\mathbf{X}}^\epsilon(t) &= [b(\tilde{\mathbf{X}}^\epsilon(t)) + \sigma(\tilde{\mathbf{X}}^\epsilon)\mathbf{u}(t, \tilde{\mathbf{X}}^\epsilon(t))]dt + \sqrt{\epsilon}\sigma(\tilde{\mathbf{X}}^\epsilon(t))d\mathbf{W}_t \\ \tilde{\mathbf{X}}^\epsilon(0) &= \mathbf{x}_0 \end{aligned}$$

Then the importance weight is

$$\frac{d\mathbb{P}}{d\mathbb{P}^u} = \exp\left\{-\frac{1}{\sqrt{\epsilon}} \int_0^{t_f} \mathbf{u}(s, \tilde{\mathbf{X}}^\epsilon(s))d\mathbf{W}_s - \frac{1}{2\epsilon} \int_0^{t_f} |\mathbf{u}(s, \tilde{\mathbf{X}}^\epsilon(s))|^2 ds\right\}. \quad (10)$$

The derivative in the importance weight is taken in the Radon-Nikodym sense.

With Girsanov's theorem we have a theoretically justified way of computing the importance weight of a biased path with respect to the nominal measure of the original system. The question now is how does one choose a proper biasing $\mathbf{u}(x, t)$ such that the resulting importance sampling estimator will be efficient. To that end, we must define what it means for an estimator to be efficient.

From classical importance sampling theory for unbiased estimators, one usually desires the variance of the estimator to be as close to zero as possible. This is equivalent to desiring the second moment of the estimator to be equal to twice the probability of interest. Such an estimator is said to be strongly efficient [4]. To obtain a distribution that has this property while still being easy to sample from is difficult [4]. Therefore, a different, looser criteria is usually prescribed. Rather than having the second moment of the importance sampling estimator be close to the square of the probability of interest, one instead designs an estimator where the large deviations decay rate of the second moment closely match twice the large deviations decay rate of the probability of interest. An estimator that has this property is called weakly or asymptotically efficient [4]. Using this property, the authors in [13] design dynamic importance sampling algorithms for a large variety of problems. We refer to [21] for a richer bibliography of the field, further details of the exact theory of the method, and details of the algorithm.

The work of [2] extends the dynamic importance sampling analysis of [13] to dynamic importance sampling of stochastic differential equations. Given a stochastic differential equation with a small noise parameter ϵ , $d\mathbf{X}^\epsilon(t) = b(\mathbf{X}^\epsilon(t))dt + \sqrt{\epsilon}\sigma(\mathbf{X}^\epsilon(t))dW(t)$, and some predefined set of interest $E \subset \mathcal{AC}([0, t_f]; \mathbb{R})$ to find the optimal biasing $\mathbf{u}(t, x)$, one first solves a Hamilton-Jacobi equation of the form

$$\begin{aligned} \frac{\partial U}{\partial t} - H(x, \nabla U) &= 0 \\ H(x, \alpha) &= -\langle b(x), \alpha \rangle + \frac{1}{2}|\sigma(x)^T \alpha|^2, \end{aligned} \quad (11)$$

then sets the optimal biasing $\mathbf{u}(x, t) = -\sigma(x)^T \nabla U(x, t)$. The initial and boundary conditions of the Hamilton-Jacobi equation will depend on the set of interest E . The choice of this biasing will result in an asymptotically efficient importance sampling estimator. Alternatively, we may solve a variational problem at every point in the simulation [2]. Define $a(x) = \sigma(x)\sigma(x)^T$. For each (x, t) , we solve the following variational problem

$$U(x, t) = \inf_{\varphi \in \mathcal{AC}[t, t_f]} \left\{ \int_t^{t_f} \frac{1}{2}(\dot{\varphi}(t) - b(\varphi(t))^T a^{-1}(\varphi(t))(\dot{\varphi}(t) - b(\varphi(t)))ds : \varphi(t) = x, \varphi \in E \right\}. \quad (12)$$

Due to the structure of stochastic differential equations, the optimal biasing at each step will be $\mathbf{u}(x, t) = \sigma^{-1}(x)(\dot{\varphi}^*(t) - b(x))$ where φ^* is the solution to Equation 12. Solving the optimization problem during the

simulation will be more efficient than precomputing the Hamilton-Jacobi equation globally, especially in high dimensional problems [2]. The integral in the problem is known as the large deviations rate function for stochastic differential equations, and the integrand is known as the local rate function [22]. Large deviations principles allow one to characterize the rarity of some set in a probabilistic model that does not require knowing the exact probabilities via a rate function. We state the main theorem from [9, 22] describing large deviations principles for stochastic differential equations as follows:

Theorem IV.2 (Freidlin-Wentzell) *Define a diffusion process as in 9. Let $a(x) = \sigma(x)\sigma(x)^T$. Then the diffusion satisfies a large deviations principle on $\mathcal{C}_0([0, T])$ with rate function*

$$I(\varphi(\cdot)) = \frac{1}{2} \int_0^T (\dot{\varphi}(s) - b(\varphi(s)))^T a^{-1}(\varphi(s))(\dot{\varphi}(s) - b(\varphi(s))) ds.$$

The stochastic differential equation satisfies an LDP with rate function I . That is, for any open set $O \subset \mathcal{C}_0([0, t_f])$

$$\liminf_{\epsilon \rightarrow 0} \epsilon \log \mathbb{P}_\epsilon(X^\epsilon \in O) \geq - \inf_{\varphi \in O} I(\varphi(\cdot))$$

and for any closed set $C \subset \mathcal{C}_0([0, t_f])$,

$$\limsup_{\epsilon \rightarrow 0} \epsilon \log \mathbb{P}_\epsilon(X^\epsilon \in C) \leq - \inf_{\varphi \in O} I(\varphi(\cdot)).$$

From this perspective, one can roughly argue that finding a good biasing path hinges on finding a ‘‘least rare’’ path to the rare event as informed by the large deviations rate function of the dynamics. Algorithm 1 summarizes the method in an idealized setting based on the approach of [2]. Next we apply this theory to the model and discuss specific aspects of the algorithm.

Algorithm 1: Optimal biasing for rare event simulation

Data: SDE Model: Equation 9, E rare event of interest

Result: Optimal biasing of one sample $\tilde{\mathbf{X}}^\epsilon(t)$, $\mathbf{u}(t, x)$

- ```

1 while $X^\epsilon \notin E$ do
2 Solve optimization problem in Equation 12, obtain optimal path $\varphi^*(s)$
3 Compute $\mathbf{u}(t_n, \mathbf{X}_n^\epsilon) = \sigma^{-1}(\mathbf{X}_n^\epsilon)(\dot{\varphi}^*(t_n) - b(\mathbf{X}_n^\epsilon))$
4 Evolve Equation 9 forward in time $t_{n+1} = t_n + \Delta t$,

$$\tilde{\mathbf{X}}_{n+1}^\epsilon = (b(\tilde{\mathbf{X}}_n^\epsilon) + \sigma(\tilde{\mathbf{X}}_n^\epsilon)\mathbf{u}(\tilde{\mathbf{X}}_n^\epsilon))\Delta t + \sqrt{\epsilon \Delta t} \sigma(\tilde{\mathbf{X}}_n^\epsilon) \Delta W_{t_n}$$


```
- 

## V. Applying the theory to the model

Based on the explorations of the model and its instabilities in Section III, we wish to estimate the probability that the vehicle pitch angle exceeds  $\pm 15^\circ$  within a time window of 10 seconds, while the pilot has initially trimmed the rotorcraft so that it is level with the ground  $\theta(0) = 0^\circ$ . This roughly corresponds to the probability that the tail fin stalls in flight and causes instabilities within 10 seconds before the pilot can react and trim the helicopter for stability. Note that there is no additional control applied by any autonomous system or by the pilot in the 10 second period. The system is evolving on its own according to its dynamics under stochastic forcing from the noisy wind. Define  $E$  to be

$$E = \{\theta(t) | \exists t^* \in [0, 10], |\theta(t^*)| \geq 15^\circ\} \subset \mathcal{AC}([0, 10]; \mathbb{R}).$$

We model the noise in the wind as an Ornstein-Uhlenbeck process with  $\mathbf{V}_0 = [44.2, 0]^T$  m/sec,  $\sigma_x = 0.89$  m/sec and,  $\sigma_z = 1.56$  m/sec. We first find the large deviations rate function of the system. Since the stochastic part of the model is only in the wind, the large deviations rate function of the system is captured by the Ornstein-Uhlenbeck process alone. Therefore we have that

$$\mathcal{L}(\mathbf{V}, \dot{\mathbf{V}}) = \frac{1}{2}((\mathbf{V} - \mathbf{V}_0) + \dot{\mathbf{V}})^T (\sigma \sigma^T)^{-1} ((\mathbf{V} - \mathbf{V}_0) + \dot{\mathbf{V}}) \quad (13)$$

if the deterministic model is satisfied and is equal to infinity otherwise. To find the optimal biasing for the wind at any location and time  $(x, t)$ , we need to solve the following family of variational problems

$$U(x, t) = \inf_{\mathbf{V} \in \mathcal{AC}([t, t_f]; \mathbb{R})} \left\{ \int_t^{t_f} \frac{1}{2} ((\mathbf{V} - \mathbf{V}_0) + \dot{\mathbf{V}})^T \sigma^{-2} ((\mathbf{V} - \mathbf{V}_0) + \dot{\mathbf{V}}) ds : \begin{bmatrix} \dot{\theta} \\ \dot{q} \\ \dot{\mathbf{V}} \end{bmatrix} = \begin{bmatrix} q \\ \frac{1}{I_y} M_{CG}(\theta, \mathbf{V}(t)) \\ (\mathbf{V} - \mathbf{V}_0) + \sigma \mathbf{u} \end{bmatrix}, \theta(t) \in E \right\}. \quad (14)$$

Via the contraction principle from large deviations theory [9], we can re-write the optimization problem as an optimal control problem

$$U(x, t) = \inf_{\mathbf{u} \in \mathcal{AC}[0, t]} \left\{ \int_t^{t_f} \frac{1}{2} \|\mathbf{u}(s)\|^2 ds : \begin{bmatrix} \dot{\theta} \\ \dot{q} \\ \dot{\mathbf{V}} \end{bmatrix} = \begin{bmatrix} q \\ \frac{1}{I_y} M(\theta, \mathbf{V}(t)) \\ (\mathbf{V} - \mathbf{V}_0) + \sigma \mathbf{u} \end{bmatrix}, \theta(t) \in E \right\}. \quad (15)$$

Intuitively, one can view this algorithm as taking control of the noise term in the model and finding a biasing path that is the “least rare” way that will cause the dynamics to go towards the rare event of interest. With a biasing path, we can find the importance weight between paths with Girsanov’s theorem. Note that in this problem, we have incorporated  $\epsilon$  into  $\sigma$ . Let the importance weight computed from Equation 10 be

$$Z_E = \exp \left( - \int_0^{t_f} \langle \mathbf{u}(t), d\mathbf{W}(t) \rangle - \frac{1}{2} \int_0^{t_f} \|\mathbf{u}(t)\|^2 dt \right). \quad (16)$$

Then the importance sampling estimator we obtain is

$$\hat{\rho}_E = \frac{1}{K} \sum_{i=1}^K \mathbb{1}_E(\theta^i(\cdot)) Z_E^i \quad (17)$$

where  $K$  the number of independent sample paths.

We can solve the optimization problem numerically in a brute force fashion, or we can turn this problem into a linear quadratic regulator (LQR) problem by considering a linearization. Since the length of the tail is usually chosen to stabilize the rotorcraft, the net pitching moment is dominated by the moment from the tail lift. Furthermore, since the lift generated by the tail is linear with the angle of attack, we find that a linearized model is sufficient for the purposes of solving the optimization problem. That is, we have a simple harmonic oscillator that can model the dynamics of the helicopter that is linearized around a stable equilibrium point. While using this surrogate model may not exactly give us the optimal biasing, the resulting estimator will still be unbiased. Similar approaches have been considered in [23, 24] where the authors find near-optimal biasing for nonlinear dynamical systems by first considering a linearization. In Figure 6, we plot the exact net pitching moment as a function of the pitch angle  $\theta$  with constant freestream velocity  $\mathbf{V} = [44.2, 0]^T$  m/sec. We also plot a linear approximation to the model about the equilibrium point.

Note that the resulting problem is different from the standard LQR form. Usually, one wishes to find a control that drives the system towards zero. In our scenario, we wish to drive the system to a particular point. To solve our optimal control problem, we use a modified LQR algorithm presented in [25] to find the optimal biasing  $\mathbf{u} = [u_x, u_z]^T$  at each time step. Note that we can replace  $\mathbf{V}$  with the variable  $\tilde{\mathbf{V}} = \mathbf{V} - \mathbf{V}_0$ . Let  $\mathbf{u} = [u_x, u_z]^T$ . For the model at hand, after linearization, we can obtain an LQR problem of the following form

$$\tilde{U}(x, t) = \inf_{\mathbf{u} \in \mathcal{AC}[t, t_f]} \left\{ \int_t^{t_f} \frac{1}{2} \|\mathbf{u}(s)\|^2 ds : \begin{bmatrix} \dot{\theta} \\ \dot{q} \\ \dot{\tilde{V}}_x \\ \dot{\tilde{V}}_z \end{bmatrix} = \begin{bmatrix} 0 & 1 & 0 & 0 \\ a & 0 & b & c \\ 0 & 0 & -1 & 0 \\ 0 & 0 & 0 & -1 \end{bmatrix} \begin{bmatrix} \theta \\ q \\ \tilde{V}_x \\ \tilde{V}_z \end{bmatrix} + \begin{bmatrix} 0 & 0 & 0 & 0 \\ 0 & 0 & 0 & 0 \\ 0 & 0 & \sigma_x & 0 \\ 0 & 0 & 0 & \sigma_z \end{bmatrix} \begin{bmatrix} 0 \\ 0 \\ u_x \\ u_z \end{bmatrix}, \theta(t) = x, \theta \in E \right\}. \quad (18)$$

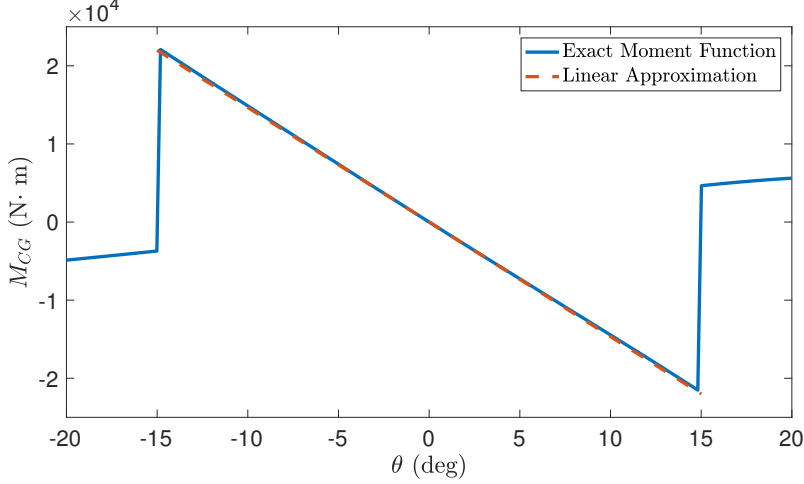


**Fig. 6** We plot the net moment as a function of the pitch angle  $\theta$  with the zero noise in the wind and assuming the system is cruising at a velocity of  $\mathbf{V} = [44.2, 0]^T$  m/sec.

where  $a, b, c < 0$ .

Since the exact time  $t^*$  that a least rare path enters the rare event may be change as a simulation is happening, and because the rare event region is split into two parts, there is an outer optimization loop to the problem in Equation 18. The outer optimization loop finds  $t^*$  and finds which direction the method should bias towards  $+15^\circ$  or  $-15^\circ$ . Finally, to make our problem more similar to the standard LQR algorithm, the endpoint constraint is replaced by a quadratic terminal penalty with a large constant. A more precise formulation of 18 is given as follows:

$$\tilde{U}(x, t) = \inf_{\substack{t^* \in [t, t_f] \\ \theta_f \in \{-15^\circ, 15^\circ\} \\ \mathbf{u} \in \mathcal{AC}[t, t^*]}} \left\{ \frac{1}{2} C_K (\theta(t^*) - \theta_f)^2 + \int_t^{t^*} \frac{1}{2} \|\mathbf{u}(s)\|^2 ds : \begin{bmatrix} \dot{\theta} \\ \dot{q} \\ \dot{\tilde{V}_x} \\ \dot{\tilde{V}_z} \end{bmatrix} = \begin{bmatrix} 0 & 1 & 0 & 0 \\ a & 0 & b & c \\ 0 & 0 & -1 & 0 \\ 0 & 0 & 0 & -1 \end{bmatrix} \begin{bmatrix} \theta \\ q \\ \tilde{V}_x \\ \tilde{V}_z \end{bmatrix} + \begin{bmatrix} 0 & 0 & 0 & 0 \\ 0 & 0 & 0 & 0 \\ 0 & 0 & \sigma_x & 0 \\ 0 & 0 & 0 & \sigma_z \end{bmatrix} \begin{bmatrix} u_x \\ u_z \end{bmatrix}, \theta(t) = x \right\}, \quad (19)$$

where  $C_K > 0$  is a large constant. We give the concrete algorithm we implement in Algorithm 2.

---

**Algorithm 2:** Obtain rare event probability estimate

---

**Data:** Linearized model in Equation 18, exact SDE model in Equation 15, Number of desired samples

$K$ , Rare event of interest  $E$

**Result:** Probability estimate  $\hat{\rho}_E$

- ```

1 for  $i = 1$  to  $K$  do
2   while  $\theta \notin E$  do
3     | Solve optimization problem in Equation 19 via an LQR algorithm, find  $\mathbf{u}(t)$ , evaluate at  $t_n$ .
4     | Evolve exact SDE model one time step with biasing  $\mathbf{u}(t_n)$ 
5     | Compute importance weight  $Z_E^i = \exp\left(-\int_0^{t^*} \langle \mathbf{u}(t), d\mathbf{W}_t \rangle - \frac{1}{2} \int_0^{t^*} \|u(t)\|^2 dt\right)$ .
6 return  $\hat{\rho}_E = \frac{1}{K} \sum_{i=1}^K \mathbb{1}_E(\theta(t)) Z_E^i$ 

```
-

In Figure 7, we show seven plots relating to a biased sample of the rotorcraft model. The first plot shows the evolution of θ over time. We see that the path enters the rare event around $t = 8.6s$. In the second and third plots, we show the corresponding noisy wind that causes the rare event. In the fourth and fifth plots, we show the optimal control of the noise of the wind that leads to the rare event. We see that the control is

oscillatory, which makes sense. One can think of the analogy of a playground swing, where one pushes the system at the correct times to force the θ to grow over time. In the sixth plot, we show the target final time, which changes over the course of the simulation. In the seventh plot, we show which direction the biasing pushes towards, which changes over the course of the simulation. As expected, this plot is roughly periodic as well since the path approaches the two sides of the rare event periodically.

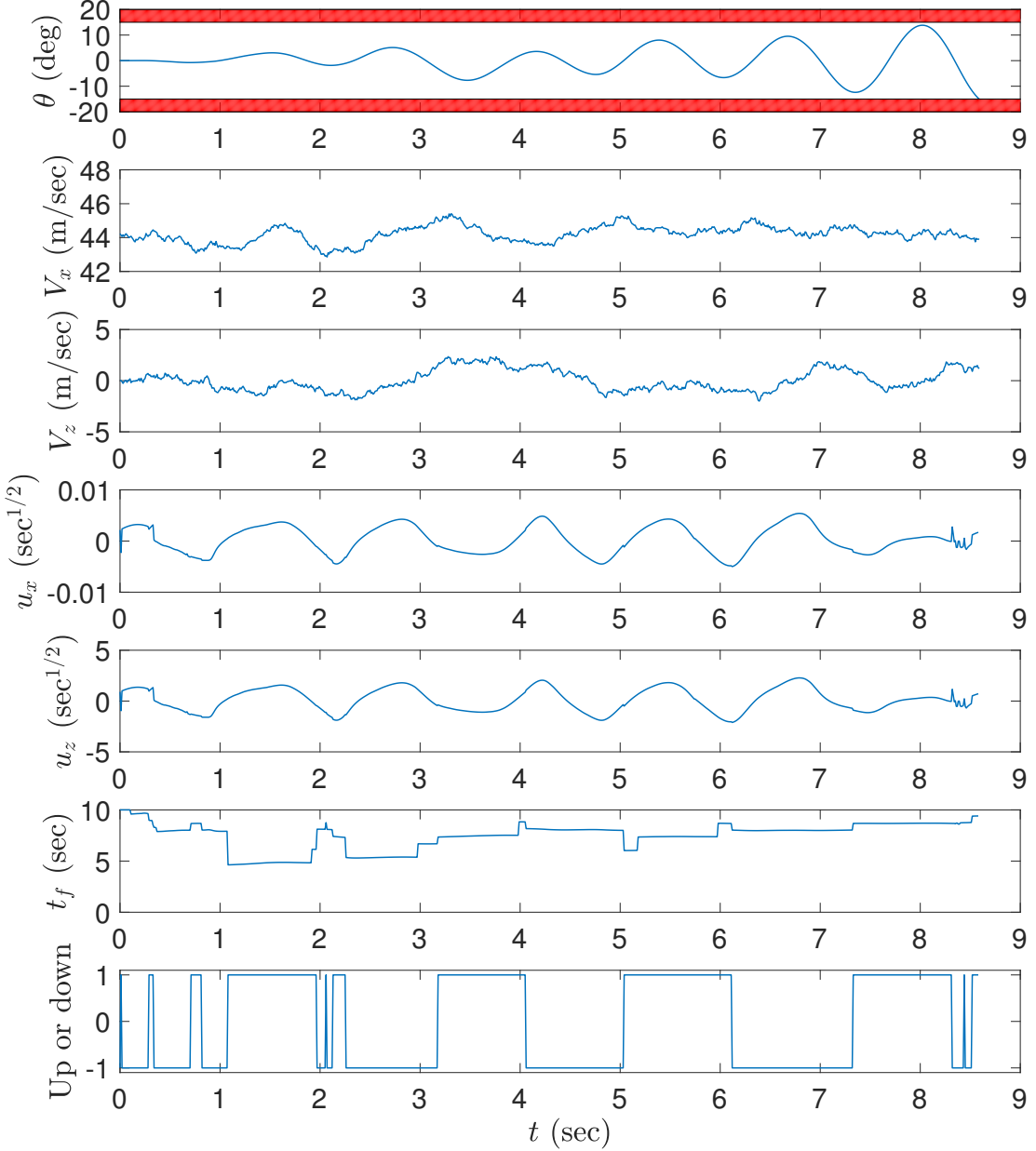


Fig. 7 An example of a biased sample of the rotorcraft model that reaches the rare event by time $t = 8.6s$. The top three figures show the pitch angle and the velocity profile of the aircraft with noisy wind. The fourth and fifth figures show the applied biasing through time. The sixth figure shows the estimated end time in the rare event as the simulation is occurring. The seventh figure shows whether the algorithm is biasing towards $+15^\circ$ or -15° . The simulation ends when the pitch angle reaches the rare event.

In Figure 8, we show 50 simple Monte Carlo samples of the rotorcraft system – i.e. *without* biasing – including the corresponding realizations of the wind velocities. Note that no samples reach the rare event.

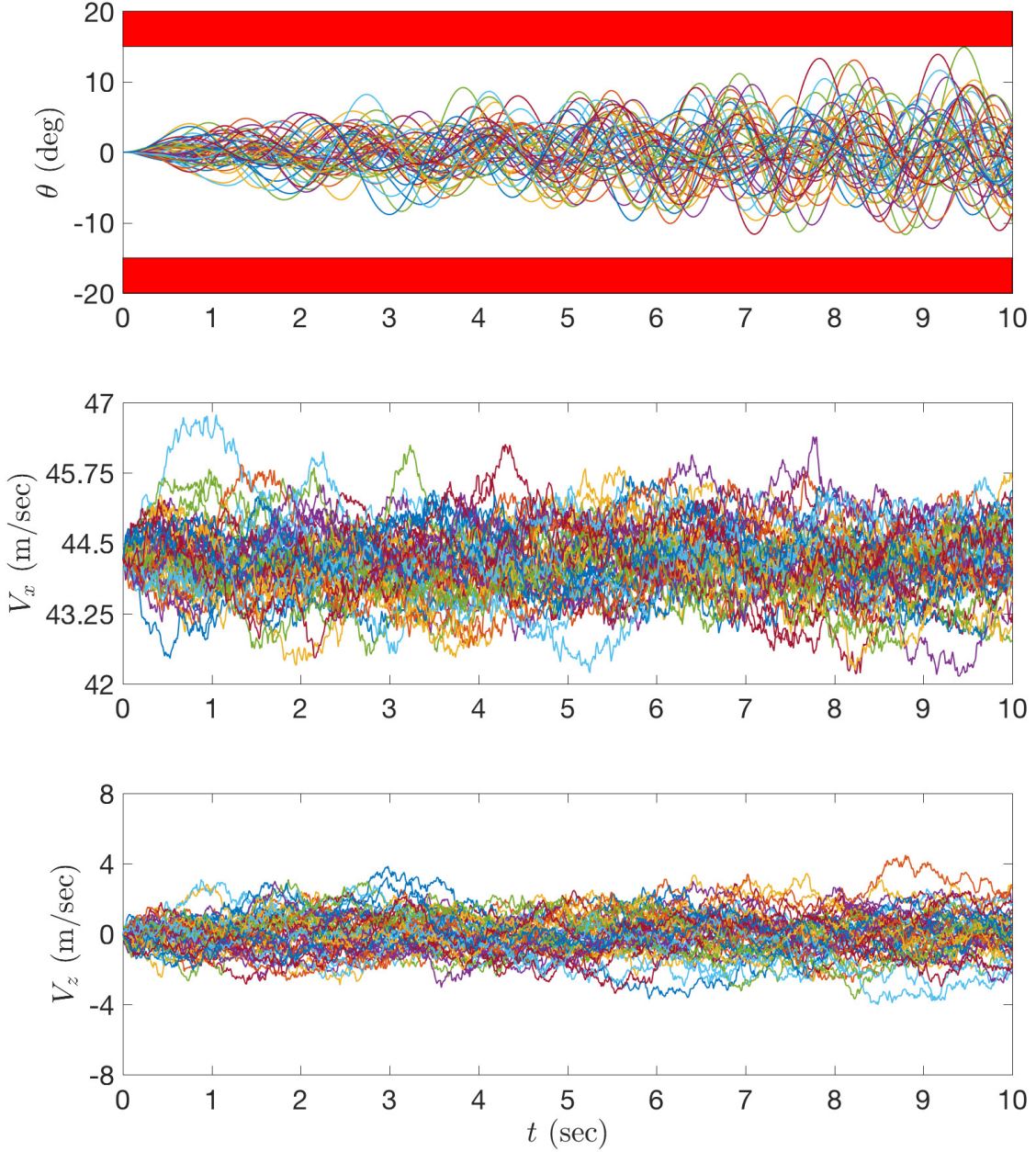


Fig. 8 Simple or unbiased Monte Carlo samples of the rotorcraft model.

In Figure 9, we show 50 biased samples. It seems that all paths lead to the rare event, but not all paths to the rare event are equally important. In Figure 10 we shade each path according to its importance weight relative to the least rare path of the batch.

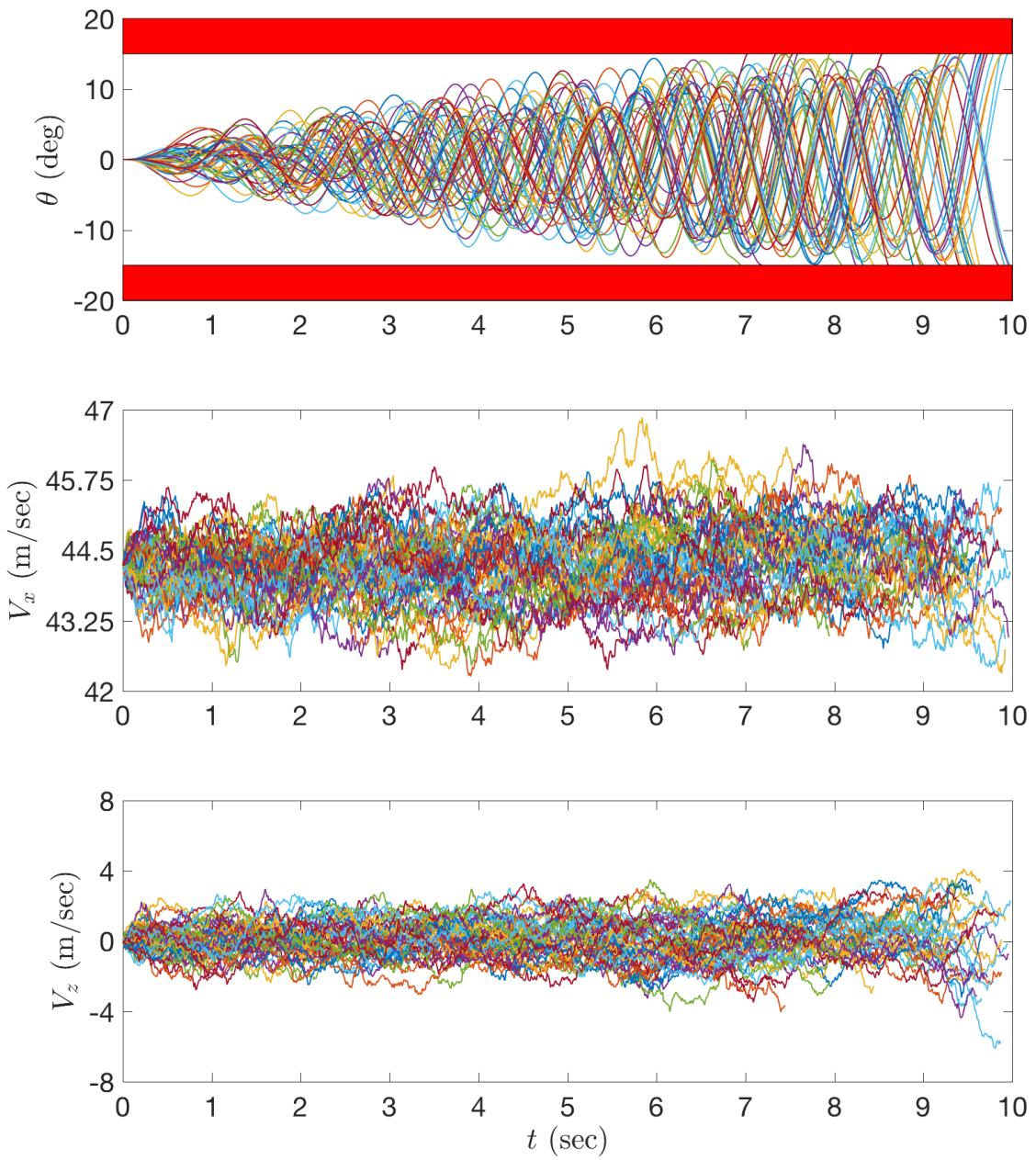


Fig. 9 Biased samples of the model.

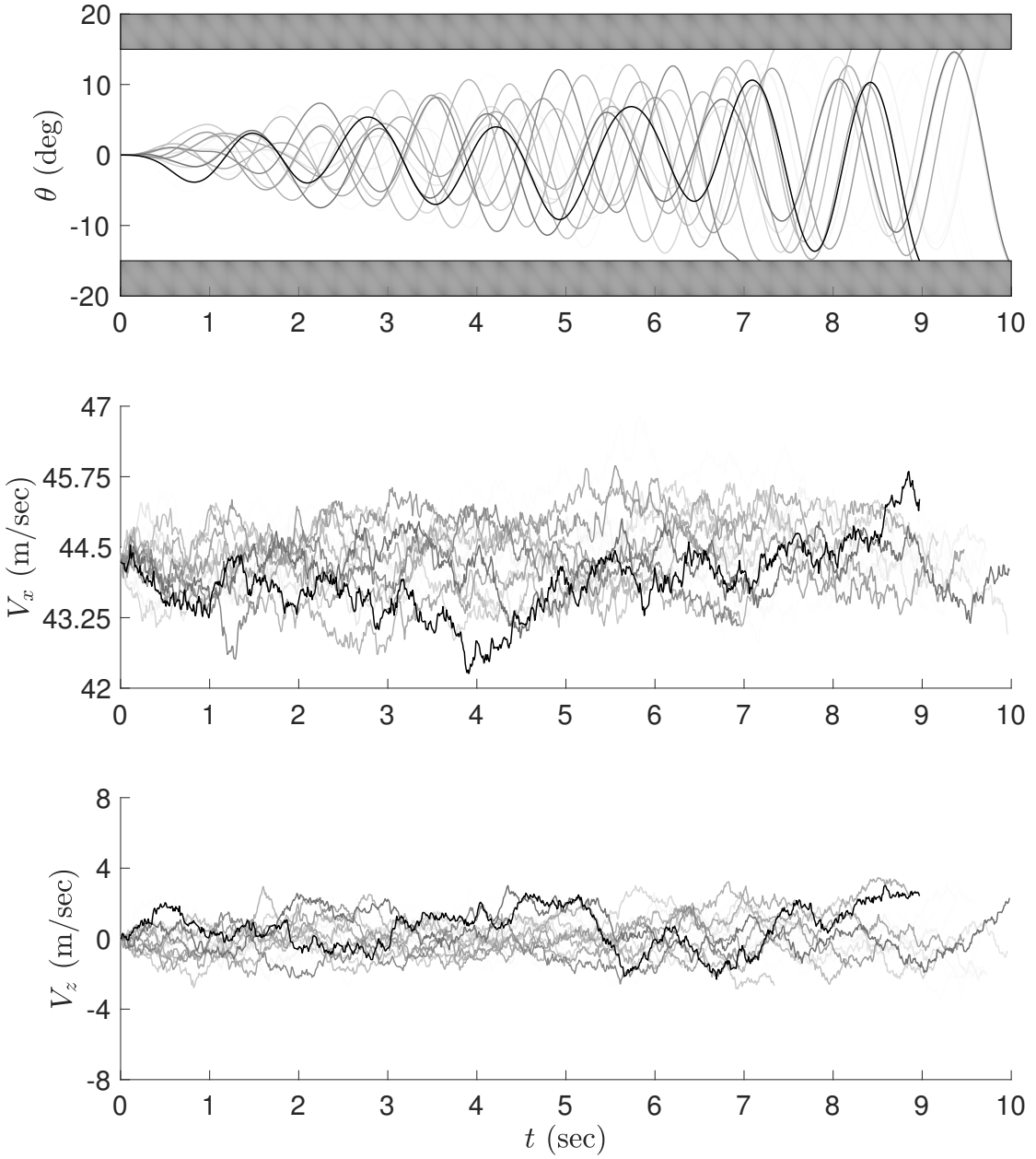


Fig. 10 Weighted biased samples. Each path from Figure 9 is shaded according to its importance weight relative to the path with the largest weight in the batch.

Finally, we state the computed probabilities based on simple Monte Carlo and dynamic importance sampling. We take the true probability to be estimated by simple Monte Carlo with 1.5 million sample paths, $\rho_{true} = 7.83 \times 10^{-3}$. The following probabilities are computed with 100 batches of 1000 samples for each method.

Table 2 Rotorcraft example results

n	Estimate $\hat{\rho}_n$	Std. Error	95% confidence	Relative error	Rel. error per sample
MC	7.80×10^{-3}	8.23×10^{-3}	$[0, 24.3] \times 10^{-3}$	1.06	33.5
DIS	7.77×10^{-3}	1.33×10^{-3}	$[5.11, 10.43] \times 10^{-3}$	0.17	5.40

We observe significant variance reduction, as evidenced by a roughly seven-fold reduction in relative error per sample and a narrower 95% confidence interval that places a meaningful lower bound on the failure probability. That said, the amount of variance reduction we observe for this problem is not as great as has been reported in other literature on dynamical importance sampling [2, 13]. One issue that diminishes the performance of the method is identified in [23]: the efficiency of dynamic importance sampling for small noise diffusions can deteriorate in the presence of an attractor. Our problem has an attractor, since the system is oscillating around an equilibrium point and because of the mean reverting nature of the wind. The authors in [23] note an improvement of the algorithm by considering the noise level ϵ into account when finding the optimal biasing; however, their approach does not extend to higher dimensions. In [26], the authors present an approach that applies to higher-dimensional problems; their algorithm, however, requires the system dynamics to be linear and self-adjoint. The latter condition, in particular, is not satisfied by the helicopter model considered here. Therefore, these fixes do not yet seem theoretically viable for real engineering problems.

VI. Conclusion

We applied a state-of-the-art method for rare event simulation of small noise diffusions [2] to a computational model of a rotorcraft system. We consider the rare event that the magnitude of the rotorcraft pitch angle exceeds some value within a fixed time interval, in the presence of stochastic forcing from the wind. One goal of this paper is to introduce the engineering community to rare event simulation techniques with theoretical efficiency guarantees, and to show that they can be successfully applied to systems of interest. We noted that while our method does reduce the variance of the estimator, it does not perform as well as claimed in dynamic importance sampling literature. This phenomenon has been well noted and is due to the presence of an attractor in the system dynamics. Future work should consider finding theoretically sound adaptations of the algorithms in [23] and [26] to more realistic settings for engineering problems.

We may also explore modeling the wind with higher fidelity models such as the Dryden and von Kármán wind turbulence models [27], which are approved by the Department of Defense for designing aircraft systems. Using these models may pose a further theoretical challenge; [28] has noted that the von Kármán wind turbulence model can be derived from a fractional Ornstein-Uhlenbeck process, which is not compatible with our current methodology.

We may also consider further rare events caused by parametric uncertainty in the design parameters of the rotorcraft system. Lastly, we may also apply work related to data assimilation of rare events [2] to the rotorcraft system, for the online prediction of rare events.

VII. Acknowledgment

This material is based upon work supported by the DARPA EQUiPS program and by the United States Air Force under Contract No. FA8650-16C-7646. Any opinions, findings and conclusions or recommendations expressed in this material are those of the author(s) and do not necessarily reflect the views of the United States Air Force.

References

- [1] Vanden-Eijnden, E., and Weare, J., “Data assimilation in the low noise regime with application to the Kuroshio,” *Monthly Weather Review*, Vol. 141, No. 6, 2013, pp. 1822–1841.
- [2] Vanden-Eijnden, E., and Weare, J., “Rare event simulation of small noise diffusions,” *Communications on Pure and Applied Mathematics*, Vol. 65, No. 12, 2012, pp. 1770–1803.
- [3] Bucklew, J. A., *Introduction to Rare event Simulation*, Springer Series in Statistics, Springer, New York, 2004.
- [4] Asmussen, S., and Glynn, P. W., *Stochastic Simulation: Algorithms and Analysis*, Vol. 57, Springer Science & Business Media, 2007.
- [5] Owen, A. B., *Monte Carlo Theory, Methods and Examples*, 2013.
- [6] Asmussen, S., and Binswanger, K., “Simulation of ruin probabilities for subexponential claims,” *Astin Bulletin*, Vol. 27, No. 02, 1997, pp. 297–318.
- [7] Rubinstein, R. Y., and Kroese, D. P., *The cross-entropy method: a unified approach to combinatorial optimization, Monte-Carlo simulation and machine learning*, Springer Science & Business Media, 2013.
- [8] Li, J., and Xiu, D., “Computation of failure probability subject to epistemic uncertainty,” *SIAM Journal on Scientific Computing*, Vol. 34, No. 6, 2012, pp. A2946–A2964.
- [9] Dembo, A., and Zeitouni, O., *Large Deviations Techniques and Applications*, Vol. 38, Springer Science & Business Media, 2009.
- [10] Dupuis, P., and Ellis, R. S., *A Weak Convergence Approach to the Theory of Large Deviations*, Vol. 902, John Wiley & Sons, 2011.
- [11] Varadhan, S. S., *Large Deviations and Applications*, SIAM, 1984.
- [12] Siegmund, D., “Importance sampling in the Monte Carlo study of sequential tests,” *The Annals of Statistics*, 1976, pp. 673–684.
- [13] Dupuis, P., and Wang, H., “Importance sampling, large deviations, and differential games,” *Stochastics: An International Journal of Probability and Stochastic Processes*, Vol. 76, No. 6, 2004, pp. 481–508.
- [14] Min, B.-Y., “A physics based investigation of Gurney flaps for enhancement of rotorcraft flight characteristics,” Ph.D. thesis, Georgia Institute of Technology, 2010.
- [15] Johnson, W., *Helicopter Theory*, Courier Corporation, 2012.
- [16] Leishman, G. J., *Principles of Helicopter Aerodynamics*, Cambridge university press, 2006.
- [17] Taylor, J. W. R., et al., *Jane’s All the World’s Aircraft*, Jane’s, 1981.
- [18] Zárate-Miñano, R., Anghel, M., and Milano, F., “Continuous wind speed models based on stochastic differential equations,” *Applied Energy*, Vol. 104, 2013, pp. 42–49.
- [19] Higham, D. J., “An algorithmic introduction to numerical simulation of stochastic differential equations,” *SIAM Review*, Vol. 43, No. 3, 2001, pp. 525–546.
- [20] Oksendal, B., *Stochastic Differential Equations: An Introduction with Applications*, Springer Science & Business Media, 2013.
- [21] Zhang, B. J., “A Coupling Approach to Rare Event Simulation via Dynamic Importance Sampling,” Master’s thesis, Massachusetts Institute of Technology, Cambridge, MA, 2017.
- [22] Freidlin, M. I., and Wentzell, A. D., “Random Perturbations,” *Random Perturbations of Dynamical Systems*, Springer, 1984, pp. 15–43.
- [23] Dupuis, P., Spiliopoulos, K., Zhou, X., et al., “Escaping from an attractor: Importance sampling and rest points I,” *The Annals of Applied Probability*, Vol. 25, No. 5, 2015, pp. 2909–2958.

- [24] Hartmann, C., Schütte, C., and Zhang, W., “Model reduction algorithms for optimal control and importance sampling of diffusions,” *Nonlinearity*, Vol. 29, No. 8, 2016, p. 2298.
- [25] Goretkin, G., Perez, A., Platt, R., and Konidaris, G., “Optimal sampling-based planning for linear-quadratic kinodynamic systems,” *Robotics and Automation (ICRA), 2013 IEEE International Conference on*, IEEE, 2013, pp. 2429–2436.
- [26] Salins, M., and Spiliopoulos, K., “Rare event simulation via importance sampling for linear SPDE’s,” *Stochastics and Partial Differential Equations: Analysis and Computations*, 2016, pp. 1–39.
- [27] “Flying Qualities of Piloted Aircraft,” Tech. rep., MIL-STD-1797A, Department of Defense, 1990.
- [28] Li, M., and Leng, J., “On von Kármán spectrum from a view of fractal,” *Waves, Wavelets and Fractals*, Vol. 1, No. 1, 2015.